

Roll-up effect of sulfur dioxide adsorption on zeolites FAU 13X and LTA 5A

Guanghai Li¹ · Qishuai Wang¹ · Tao Jiang¹ · Jun Luo¹ · Mingjun Rao¹ · Zhiwei Peng¹

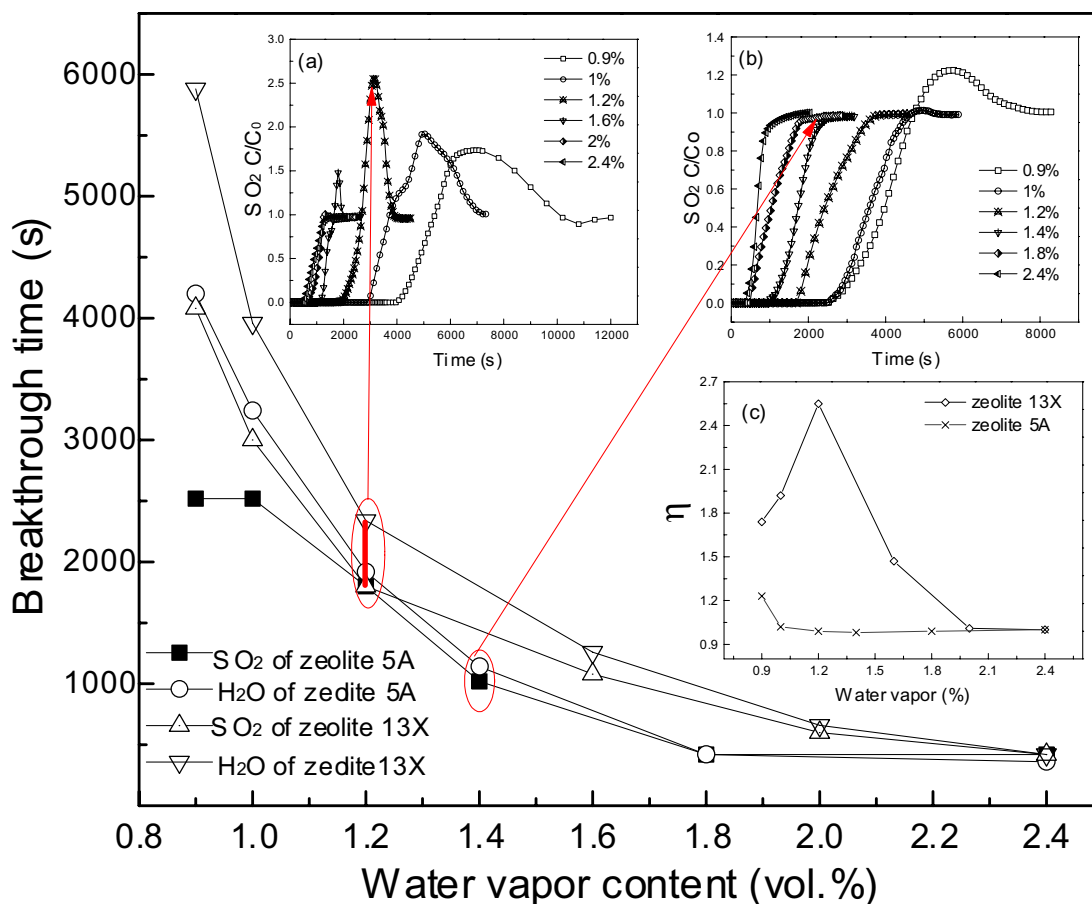
Received: 17 January 2017 / Revised: 4 April 2017 / Accepted: 5 April 2017 / Published online: 19 April 2017
© Springer Science+Business Media New York 2017

Abstract The roll-up effect occurs as a result of the displacement of SO₂ with H₂O(g) when sulfur dioxide from humid flue gas is adsorbed by zeolites. It is mainly affected by SiO₂/Al₂O₃ ratio (S/A) of zeolites, despite lack of detailed studies on use of hydrophilic zeolite. In this study, two zeolites of FAU 13X (S/A of 1.77) and LTA 5A (S/A of 1.51) were used to explore their roll-up effects using the breakthrough curve method. It is shown that the zeolite structure significantly influences the roll-up effect. The roll-up effect of FAU 13X is more significant than that of LTA 5A at the same water vapor content. The maximum

roll-up ratio (η) for LTA 5A and FAU 13X are, respectively, 1.23 and 2.55 within the water vapor content range of 0.9–2.4%. Moreover, η of FAU 13X tends to decrease more rapidly than that of LTA 5A with increasing temperature or decreasing adsorption gas pressure. The presence of oxygen inhibits the roll-up effect and increases the breakthrough time of SO₂. For the acid-modified zeolite, there is a positive correlation between η and concentration of Ca²⁺ or Na⁺ on zeolite surface, indicating obvious impact of cations on the roll-up effect.

✉ Jun Luo
luojun2013@csu.edu.cn

¹ School of Minerals Processing & Bioengineering, Central South University, 932 South Lushan Rd, Changsha 410083, Hunan, People's Republic of China



(a) Breakthrough curves of zeolite 13X within the water vapor content range from 0.9 to 2.4%
 (b) Breakthrough curves of zeolite 5A within the water vapor content range from 0.9 to 2.4%
 (c) The difference of roll-up ratio (η) between zeolite 13X and 5A

Keywords Zeolite · SO₂ · Roll-up effect · Adsorption

1 Introduction

SO₂ emission is an important precursor of both acid rain and smog, which pose a great threat to human health and the natural environment (Aunan and Pan 2004). It is reported that China's industrial SO₂ emission was more than 18.59 million tons in 2015 (NBS 2016). A large number of technologies have been proposed and applied for mitigating SO₂ emission, including wet flue gas desulfurization, semi-dry flue gas desulfurization, dry flue gas desulfurization and flue gas circulation sintering (Ishizuka et al. 2001; Xiong et al. 2014; Chang et al. 2011; Li et al. 2014). Due to advantages of low energy consumption, relatively simple technical preparation and alleviative waste disposal issues, dry sorption processes have attracted

intensive attention for SO₂ removal (Marcu and Sandulescu 2004).

Two categories of solid sorbents are commonly used in controlling SO₂ emissions, including non-regenerative sorbents, such as calcium oxide and magnesium oxide (Al-Harashseh et al. 2014), and regenerative sorbents, such as zeolites, silica gel, and charcoal (Zhou et al. 2012; Bruce et al. 1989). For the non-regenerative sorbents, the premature termination of the sorption process remains their major inherent drawback, due to pore blocking by layers of sulphate product (Gupta et al. 2004). Among the regenerative sorbents, zeolite is the most popular one which has been widely used in adsorption, gas separation and so on, due to its unique channel structure, high thermal stability and huge adsorption capacity (Deng et al. 2012; Sotelo et al. 2007; Mofarahi and Gholipour 2014; Izumi and Suzuki 2001).

The presence of water vapor affects the dry adsorption process of zeolite. Studies on hydrophobic zeolites showed that mordenite (MOR type) and pentasil (MFI

type) zeolites have a unique dynamic breakthrough curve called roll-up effect in the presence of water vapor (Stenger et al. 1993a, b; Tantet et al. 1995; Dunn et al. 1996; Rouf and Eić 1998; Mello and Eić 2002). The similar roll-up effect has also been found in adsorption process of zeolite in solutions (Barros et al. 2006). Once the adsorption bed becomes saturated with SO₂, the adsorbed SO₂ is spontaneously displaced (roll-up) by water driven from desorption, yielding an exhaust gas enriching SO₂. The overshooting peak increases in height with decreasing SO₂ concentration and increasing water vapor content in the feed mixture (Rouf and Eić 1998). The adsorption of SO₂ on mordenites and pentasil zeolites showed that the presence of water in the gas reduces the adsorption capacity of SO₂ to varying degrees, depending on the SiO₂/Al₂O₃ ratio (S/A) (Tantet et al. 1995).

Most previous studies focused on the roll-up effects of hydrophobic zeolites with S/A of above 20. It was revealed that the roll up effect is mainly affected by S/A (Rouf and Eić 1998). With increasing S/A, the attractive force between zeolite and SO₂ gradually converts from static electricity into the Van Der Waals force (Rouf and Eić 1998). This conversion determines the adsorption capacity of zeolite. It means that low S/A zeolites should have high adsorption capacity. Moreover, it was shown that the adsorption capacity and the affinity of SO₂ with natural zeolite samples depend mainly on the type of exchanged cations and decreased in the order Na⁺ > K⁺ > Mg²⁺ > Ca²⁺ (Sakizci et al. 2011). Therefore, it is important to study the roll-up effect of zeolite with low S/A.

In this study, large adsorption capacity zeolite 13X (Yi et al. 2012) with S/A of 1.77 and zeolite 5A (Mofarahi and Gholipour 2014) with S/A of 1.51 were used to study their roll-up effects by examining the effects of water vapor content, adsorption temperature, gas pressure, presence of oxygen and pre-modification.

2 Experimental

2.1 Materials

Zeolite (13X, 5A) pellets with the size of 2.5–5 mm were taken from the National Pharmaceutical Group Chemical Reagent Co., Ltd of China. The chemical compositions are presented in Table 1. It shows that their S/A ratios are similar. The zeolite had similar values of S/A: 1.51 for 5A and 1.77 for 13X. Besides, there is a significant difference in their cations. The zeolite 5A contained higher CaO (11.84 wt%) while zeolite 13X had higher content of Na₂O (13.39 wt%).

Table 1 Chemical composition of zeolite samples

Zeolite	5A (wt%)	13X (wt%)
Fe ₂ O ₃	0.97	1.22
Al ₂ O ₃	23.75	21.33
SiO ₂	35.75	37.79
CaO	11.84	0.94
MgO	2.08	2.05
Na ₂ O	2.95	13.39
K ₂ O	0.3	0.26

To obtain suitable breakthrough curves, the zeolite samples were crushed to particle size of 0.26–0.43 mm and then activated at 300 °C for 2 h in a muffle furnace. After activation, the zeolite samples were quickly placed in weighing bottle and cooled to room temperature in a glass plate filled with silica gel. Finally, the material was filled in an adsorption column. In order to study the effect of structure and cations on the roll-up effect, zeolite was pretreated by acid leaching.

The specific surface areas of zeolite 5A and 13X were determined by BET method. The adsorption gas was nitrogen, the adsorption temperature was 77 K, and the charge gas was helium (He). Samples were treated at 90 °C under the vacuum treatment for 1 h, then 300 °C under the vacuum treatment for 10 h. The nitrogen adsorption-desorption isotherms of the 13X and 5A samples are shown in Fig. 1.

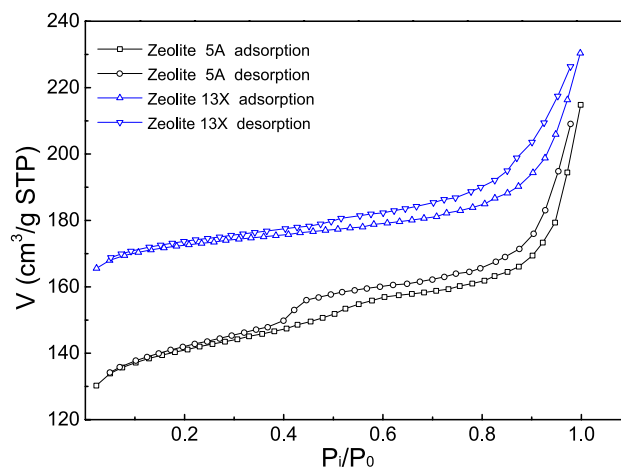


Fig. 1 N₂ adsorption–desorption isotherms of the zeolites

Table 2 The textural parameters of zeolite samples

Zeolite	13X	5A
Specific surface area (m ² g ⁻¹)	472	411
Total pore volume (cm ³ g ⁻¹)	0.27	0.33
Micropore volume (cm ³ g ⁻¹)	0.21	0.15
Average pore diameter (nm)	2.82	2.31

It shows that both materials present a type H4 isotherm (Sing 1985). The textural properties of 5A and 13X are presented in Table 2. It shows that the specific surface areas of zeolite 5A and 13X were 411 and 472 m²/g, respectively. Although zeolite 5A has a larger total pore volume, the average pore diameter and the micropore volume of 13X are greater than those of 5A.

The pore distribution of zeolite 5A and 13X was determined by BJH method. The results in Fig. 2 show that both zeolites are rich in microporous structure and LTA 5A contains a small amount of mesoporous structure. The data of specific surface area and pore distribution reveals that FAU 13X has more microporous than LTA 5A.

2.2 Methods

2.2.1 Experimental procedure

The experimental apparatus is shown in Fig. 3. The adsorption test was conducted in a U-type tube with a diameter of 10 mm, a layer of nickel foam (diameter less than or equal to 0.5 mm) which was placed at the bottom of tube and another layer of nickel foam which was also placed after charging to fix the bed. The detection system mainly consisted of two parts: determination of SO₂ and relative humidity. The gas of SO₂ was detected by enhanced type flue gas analyzer (MGA-5, YORK Instrument Ltd., Germany), and the measurement accuracy of the SO₂ is ±1 ppm. The analyzer MGA-5 was connected with the exhaust end of the fixed bed and part of the outlet gas was pumped into the flue gas analyzer for analysis, and the data were transferred to the computer and recorded. Besides, the relative humidity was detected by the temperature and humidity recorder and the measurement accuracy of relative humidity and temperature was ±2% RH and 0.1 °C,

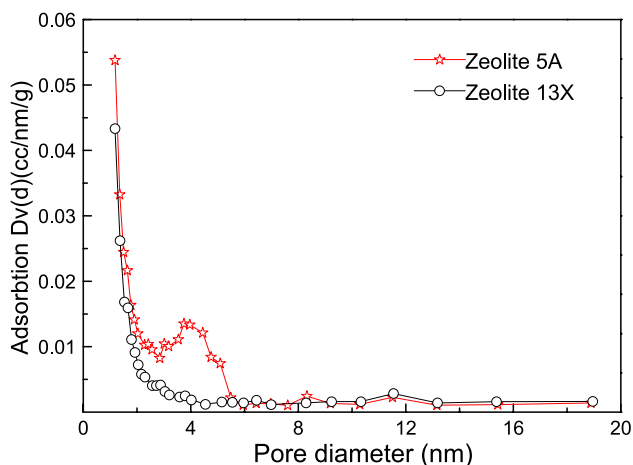


Fig. 2 Pore distribution of the zeolites

respectively. The outlet gas was mainly absorbed using a washing bottle contained sodium hydroxide solution.

At the beginning of the experiment, the cylinders with the mass flow meters were controlled for certain gas mixing. The gas was mixed evenly in the mixing chamber and the mixed gas bypassed the fixed bed before the gas concentration and relative humidity were detected. When low water vapor content needed, the nitrogen can be dried by water absorbent (silica gel). When high water vapor content needed, the nitrogen could pass through the water washing cylinder. The water vapor content was mainly controlled by the flow rate of nitrogen which had been loaded with water vapor. The concentration and relative humidity of the mixed gas were measured by the gas analyzer and the temperature and humidity recorder. Finally, the mixed gas was introduced into the fixed bed and start timing. The required adsorption temperature was controlled by a water bath (KW1000-DC). The negative pressure was provided by a vacuum pump (when needed), and the adjustment of the negative pressure was adjusted by a self-made valve with precision of 1 KPa. The pressure of the fixed bed was measured by a negative pressure meter and with the accuracy of 1 KPa. The relative humidity could be transformed into water vapor content by the software of Vaisala Humidity calculator. Then the real-time content of water vapor was detected via the temperature and humidity recorder. The time was recorded when the concentration of SO₂ in the flue gas analyzer started to rise, and the experiment was completed with stable concentration of the exhaust gas equal to the inlet SO₂ concentration.

2.2.2 Evaluation index

The adsorption property of SO₂ was determined using the breakthrough curve method, and the adsorption capacity (*A*), the breakthrough time (*t*) and the roll-up ratio (*η*) were used to characterize adsorption characteristics of zeolites.

Adsorption capacity (*A*) was defined as Eq. (1).

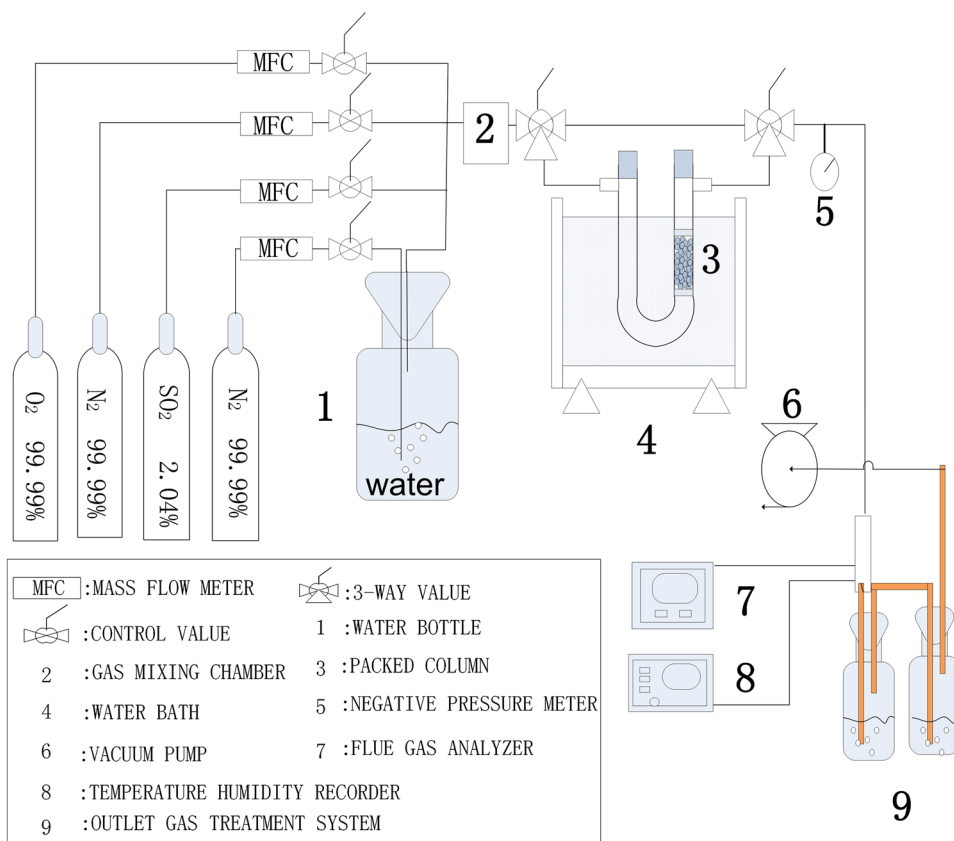
$$A = MQ \int_{t_1}^{t_2} (C_0 - C) dt / (m \cdot V_m) \quad (1)$$

where *A* is the unit zeolite mass of adsorption gas mass (mg/g); *Q* is the total gas flow rate (m³/s); *m* is the mass of the adsorbent (g); *M* is the molar mass of the adsorbed gases (g/mol); *V_m* is the standard molar volume (m³/mol); *t₁* is the start time of adsorption (s); *t₂* is the arbitrary time of adsorption process which is used as a variable in the integration process (s); *C₀* is the inlet SO₂ concentration (ppm); and *C* is the outlet SO₂ concentration at arbitrary time during the adsorption process (ppm).

Breakthrough time (*t*) was defined as Eq. (2).

$$t = t_2 - t_1 \quad (2)$$

Fig. 3 Schematic diagram of experimental apparatus for breakthrough curve measurements



where t_1 is the start time of the experiment and t_2 is the time when the concentration of the exhaust gas is equal to 1% of the inlet concentration.

Roll-up ratio (η) was defined as Eq. (3).

$$\eta = \frac{C_m}{C_0} \tag{3}$$

where C_m is the maximum outlet SO_2 concentration.

3 Results and discussion

3.1 Characterization of roll-up effect of SO_2 adsorption

3.1.1 Effect of water vapor

N_2 , SO_2 and O_2 were supplied by gas cylinders. The purity of N_2 and O_2 were 99.99 vol% and the concentration of SO_2 was 2.04 vol% balanced by N_2 . The relative humidities of N_2 , SO_2 and O_2 fluctuated between 20 and 30% at 30 °C.

The SO_2 breakthrough curves were studied under conditions: adsorbent mass 1 g, flow rate 1 L/min, SO_2 concentration 500 ppm, adsorption temperature 30 °C and at pressure 1 atm. Figure 4 shows an overshooting shape on zeolite samples under a certain water vapor content ranging from

0.9 to 2.4%. The breakthrough time of zeolite 5A decreases from 2520 to 420 s and that of zeolite 13X decreases from 4080 to 540 s, when the water vapor content increases from 0.9 to 2.4%. In addition, when the water vapor content is less than 1% for zeolite 5A and 2% for zeolite 13X, the roll-up effect appears.

Figure 5 presents an obvious difference in roll-up effect between zeolite 13X and zeolite 5A. The roll-up ratio (η) decreases from 1.23 to 1 for zeolite 5A as water vapor content increases. Moreover, the roll-up effect disappears when the water vapor content is higher than 1%. For zeolite 13X, the value of η increases first from 1.74 to 2.55 and then decreases to 1 with increasing water vapor content. Subsequently, the roll-up effect disappears when the water vapor content is higher than 2%. The results indicate that FAU 13X is more likely to generate roll-up effect compared with LTA 5A.

3.1.2 Effect of adsorption temperature

Previous studies indicated that adsorption temperature has an important effect on the adsorption of pure dry gas (Gupta et al. 2004). To clarify similar laws in the presence of water vapor on zeolite, the adsorption characteristics of SO_2 with water vapor were studied under the conditions: 1 g adsorbent, 1 L/min flow rate, 500 ppm SO_2 , 0.9% water

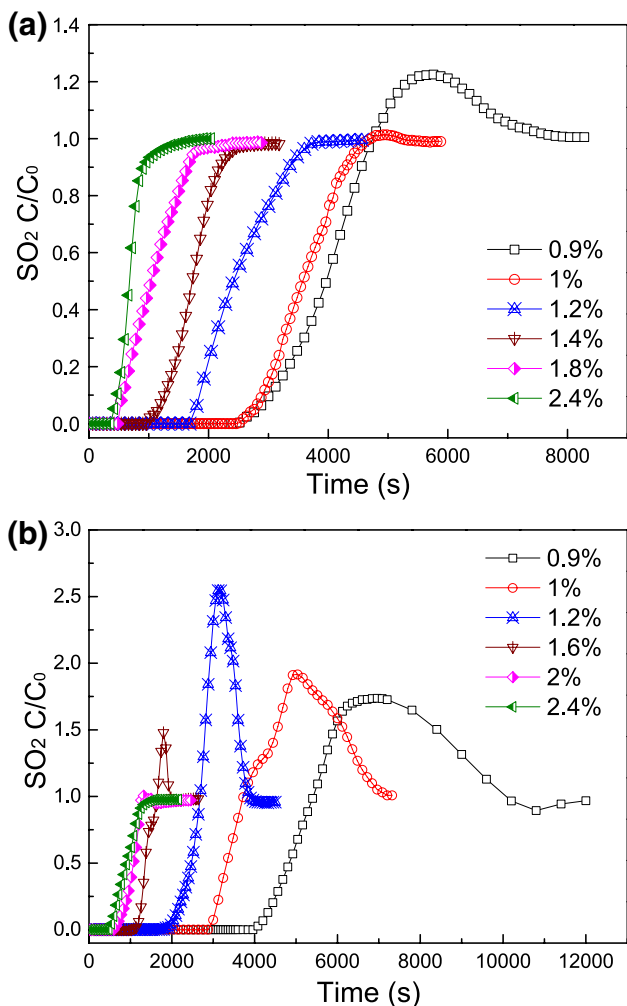


Fig. 4 Effect of water vapor content on SO₂ breakthrough curves **a** zeolite 5A; **b** zeolite 13X

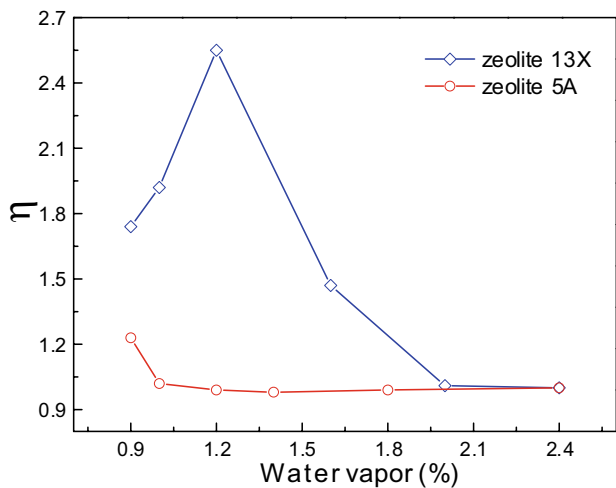


Fig. 5 Effect of water vapor on η

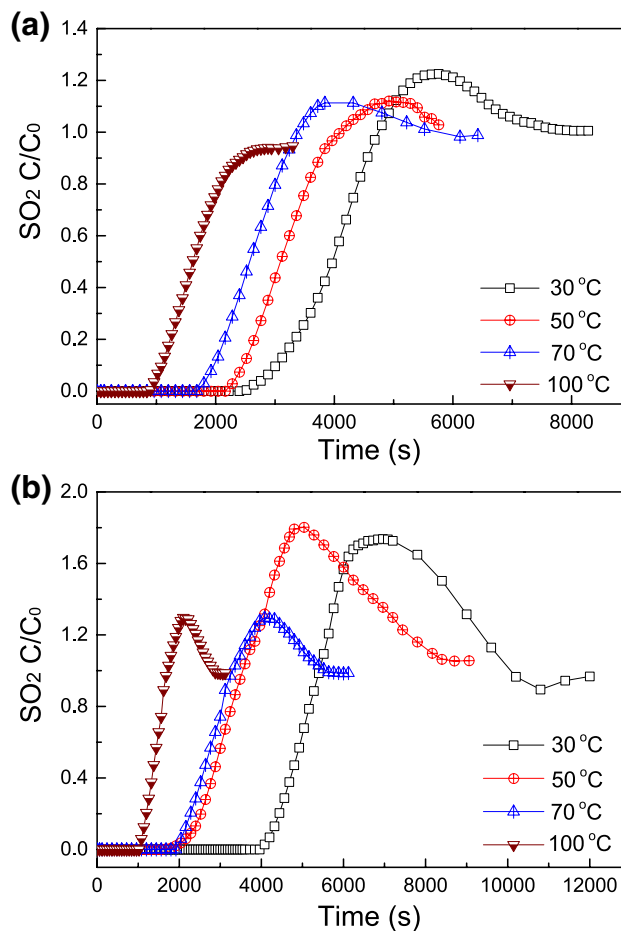


Fig. 6 Effect of adsorption temperature on SO₂ breakthrough curves **a** zeolite 5A; **b** zeolite 13X

vapor and at pressure 1 atm. Figure 6 shows that the breakthrough time is influenced strongly by adsorption temperature, and the breakthrough time gradually decreases from 2520 to 900 s (by 64%) with increasing adsorption temperature from 30 to 100 °C for zeolite 5 A. Besides, the breakthrough time decreases from 4080 to 1080 s (by 74%) with increasing adsorption temperature from 30 to 100 °C for zeolite 13X.

Figure 7 shows the trend of η at different adsorption temperatures. The η of zeolite 5A decreases from 1.23 to 1.02 (decreased by 17%) with increasing adsorption temperature from 30 to 100 °C, while the η of zeolite 13X shows an increasing trend first and then decreases, the value of η decreases from 1.74 to 1.29 (by 26%) with increasing adsorption temperature from 30 to 100 °C. This observation confirms that the adsorption temperature has greater influence on breakthrough time and roll up ratio of FAU 13X than that of LTA 5A.

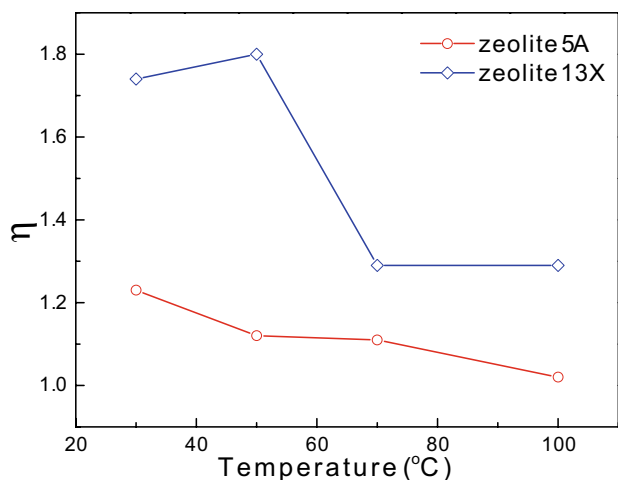


Fig. 7 Effect of temperature on η

3.1.3 Effect of gas pressure

Effect of gas pressure were studied under the conditions: 1 g adsorbent, 1 L/min flow rate, 500 ppm SO₂, adsorption temperature 30 °C, water vapor 0.9% for zeolite 5A and 1% for zeolite 13X. Figure 8 indicates that the breakthrough time decreases with the decrease of gas pressure from 1 to 0.7 atm and the breakthrough time of zeolite 5A decreases from 2400 to 1550 s, while the breakthrough time of zeolite 13X decreases from 3120 to 1920 s. The reduction of the breakthrough time by decreasing gas pressure reflects reduction in adsorption, which also caused weakened roll-up effect.

Figure 9 shows that the value of η reduces from 1.23 to 1.05 (by 15%) and from 1.92 to 1.59 (by 17%) with decreasing gas pressure from 1 to 0.7 atm for zeolite 5A and 13X, respectively. Increasing gas pressure is beneficial to roll-up effect. The gas pressure has greater influence on roll-up ratio and the breakthrough time of FAU 13X than that of LTA 5A.

3.1.4 Effect of oxygen gas

The flue gas usually contains oxygen (Zhang et al. 2012). To study the relationship between the roll-up effect and oxygen, zeolite 13X was chosen and tested at 70 and 100 °C because the roll-up effect on LTA 5A was very weak under this condition. Figure 10 shows that the presence of oxygen reduces the roll-up effect. When the oxygen content in mixture gas increases from 0 to 10% at 70 and 100 °C, the value of η decrease from 1.29 to 1.06 and from 1.26 to 1.02, respectively. The breakthrough time gradually increases from 1920 to 2040 s at 70 °C in the presence of 10% oxygen and increases from 1500 to 1680 s at 100 °C

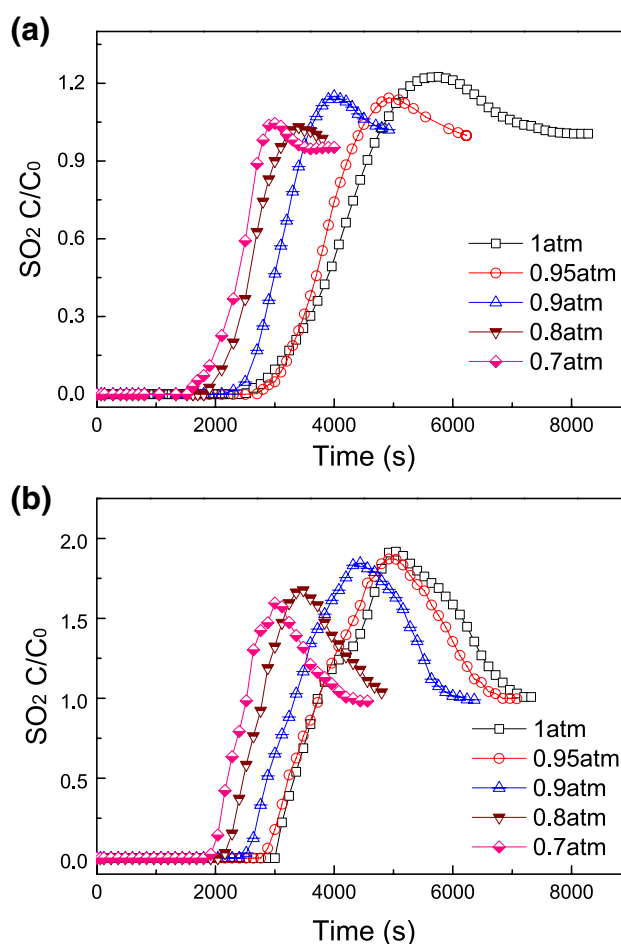


Fig. 8 Effect of gas pressure on SO₂ breakthrough curves a zeolite 5A; b zeolite 13X

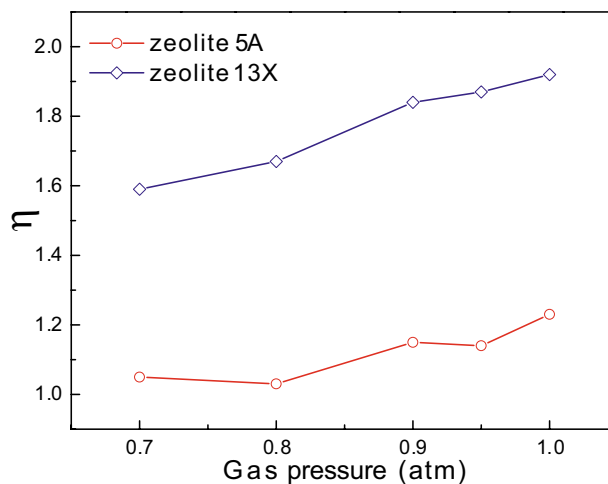


Fig. 9 Effect of gas pressure on η

in the presence of 10% oxygen. The result shows that the presence of oxygen will increase the breakthrough time and decrease the roll-up effect.

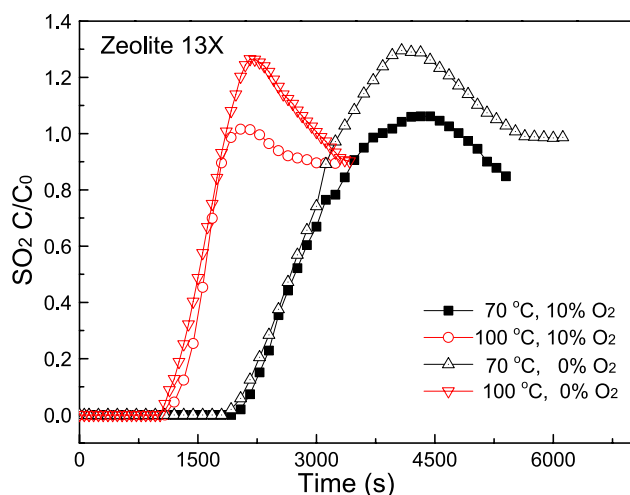


Fig. 10 Effect of oxygen on SO_2 breakthrough curves

3.2 Formation mechanisms on roll-up effect of SO_2 adsorption on zeolites

3.2.1 Competitive adsorption between SO_2 and $\text{H}_2\text{O}(\text{g})$

The roll-up effect is caused by the competition between $\text{H}_2\text{O}(\text{g})$ and SO_2 (Tantet et al. 1995). In order to explain the mechanism of generation and change of roll-up effect, the SO_2 equilibrium data was determined from the breakthrough curves using Eq. (1).

Figure 11 shows that the adsorption capacity decreases with increase of water vapor content. Meanwhile, the adsorption capacity of SO_2 increases first and then decreases to an equilibrium value. The SO_2 adsorption capacities decreases from 87.63 to 15.75 mg/g for zeolite 5A and decreases from 87.91 to 20.94 mg/g for zeolite 13X, respectively, when the adsorption finally reaches equilibrium. The existence of $\text{H}_2\text{O}(\text{g})$ leads to an obvious decrease in adsorption capacity, indicating the competition between $\text{H}_2\text{O}(\text{g})$ and SO_2 .

The relationship between breakthrough time of SO_2 and $\text{H}_2\text{O}(\text{g})$ of the zeolite is shown in Fig. 12. When the breakthrough time of $\text{H}_2\text{O}(\text{g})$ is close or essentially the same to that of SO_2 , the breakthrough curve of SO_2 is normal. When $\text{H}_2\text{O}(\text{g})$ breakthrough time is greater than that of SO_2 , the breakthrough curve presents a strange shape (seen in Fig. 4). The outlet concentration is greater than the inlet concentration and the roll-up effect appears. For example, zeolite 13X with water vapor content of 1.2% has shorter breakthrough time of SO_2 than that of $\text{H}_2\text{O}(\text{g})$, causing roll-up effect. For zeolite 5A, because the breakthrough time of SO_2 is close to that of $\text{H}_2\text{O}(\text{g})$ at water vapor content of 1.2%, the roll-up effect disappears. These phenomena

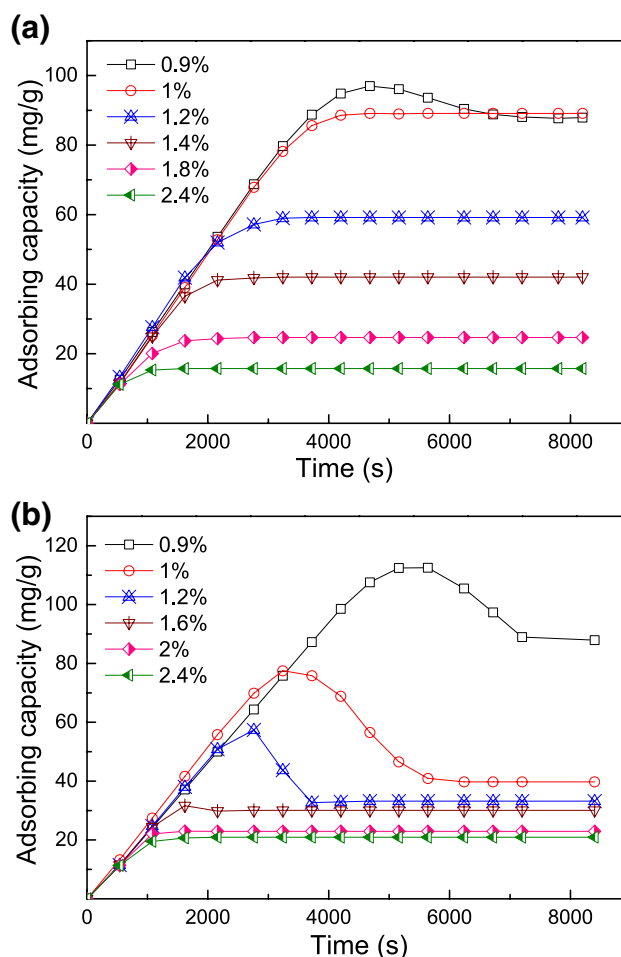


Fig. 11 Equilibrium capacities of zeolites under different water vapor contents **a** zeolite 5A; **b** zeolite 13X

further present the competitive adsorption between $\text{H}_2\text{O}(\text{g})$ and SO_2 on the zeolites. When $\text{H}_2\text{O}(\text{g})$ breakthrough rate is slower than the SO_2 breakthrough rate, the adsorption of SO_2 tended to be saturated. However, as the $\text{H}_2\text{O}(\text{g})$ adsorption continues, the $\text{H}_2\text{O}(\text{g})$ replaces a part of the adsorbed SO_2 . Due to desorption of SO_2 , the SO_2 concentration increases, presenting roll-up effect.

The SO_2 breakthrough curves in Figs. 6 and 8 shows that the η changes with different adsorption temperatures and gas pressures. These changes are associated with physical adsorption of gas. Deng et al. (2012) researched equilibrium isotherm data for SO_2 on 13X and 5A zeolite and pointed out that adsorbate molecule will contact with strong cation center on the zeolite surface first, causing immobilized molecules. When all cation centers are occupied, adsorbate molecule will be affected by a weak electric field including electric field gradient. Weak electric field were unstable and easily desorbed with decreasing gas pressure or increasing adsorption temperature. The

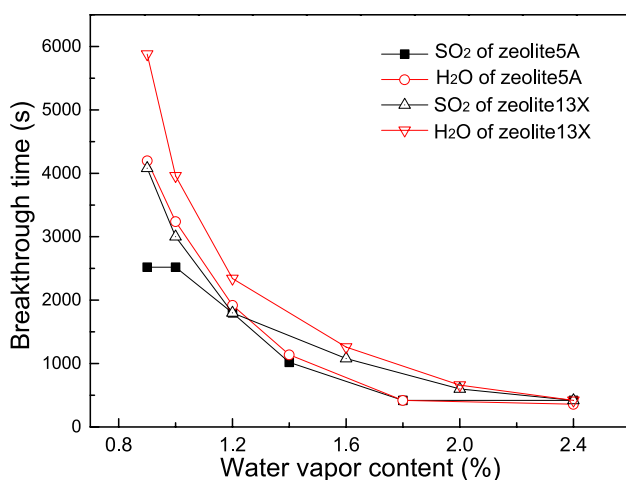


Fig. 12 Breakthrough time for different water vapor contents

unstable physical adsorption resulted in the reduction of the adsorption capacity and η .

Figure 5 shows the η of 13X increases first from 1.74 to 2.55 and then decreases to 1 with increasing water vapor content. Some researches (Stenger et al. 1993a; Rouf and Eić 1998) show that the roll-up effect is enhanced with an increase of water vapor concentration. The law could apply to the lower water vapor concentrations (0.9–1.2%) for zeolite 13X (Fig. 4). This is also in line with the data shown in Fig. 12, e.g., breakthrough times of H₂O(g) is greater or significantly greater than SO₂ for 0.9–1.2% concentration range. For zeolite 13X, only at water concentrations of 1.6% or higher the breakthrough times become very close or essentially the same to that of SO₂, which change the trend of SO₂ roll-up effects. It may be that the closeness of breakthrough times, the SO₂ can only partially saturate adsorption sites before being displaced, thus leading to reduced or no roll-up effect. For zeolite 5A, water concentrations of 0.9% or higher, the breakthrough time of water and SO₂ become more and more close, thus leading to reduced or no roll-up effect, this is also in line with the data shown in Fig. 12.

The presence of oxygen leads to a weaker roll-up effect. It might be in association with chemical adsorption. The study (Deng et al. 2012) on FAU 13X and LTA 5A found S on the surface of zeolite in form of SO₄²⁻ after adsorption, indicating potential role of the chemical adsorption. This result accounts for the reduced roll-up effect in presence of oxygen. The oxygen may elevate SO₂ chemical adsorption at high temperature. However, chemical adsorption is strong adsorption. As a result, SO₂ is difficult to be replaced by water vapor. Eventually, there is a weakened roll-up effect.

3.2.2 Effect of zeolite structure on roll-up

There are obvious differences in roll-up effect between FAU 13X and LTA 5A, although the two zeolites had close S/A ratio and specific surface area. Figures 5 and 7 show that zeolite 13X has higher roll-up ratio than 5A. Two reasons may account for this phenomenon: On one hand, FAU 13X has a larger ring window size (Yi et al. 2012) and average pore diameter than LTA 5A. Both zeolites were crystalline microporous materials with uniformed aperture size. FAU 13X has 12-oxygen ring window with a free diameter of 0.74 nm and Na⁺ balances the negative charge induced by Al³⁺, while LTA 5A has 8-oxygen ring window with a size of 0.43 nm and Ca²⁺ which balances the negative charge (Yi et al. 2012), and the average pore diameter of zeolite 13X is 2.82 nm while the average pore diameter of zeolite 5A is 2.31 nm. The kinetic diameters for SO₂, and H₂O are 0.36 and 0.30 nm, respectively. The different sizes of ring window and average pore diameter led to different space resistance when SO₂ adsorbed on zeolite and H₂O(g) replacing the adsorbed SO₂. FAU 13X has larger ring window size and average pore diameter than LTA 5A. It was easier for water vapor to replace SO₂ adsorbed on 13X than 5A. On the other hand, cations of zeolite 13X are mainly Na⁺ while cations of zeolite 5A are mainly Ca²⁺. Existing studies has shown the affinity of SO₂ follows a decreasing order as Na⁺ > K⁺ > Mg²⁺ > Ca²⁺ (Sakizci et al. 2011). The two aspects are why different amounts of SO₂ can be replaced and thereby the roll-up effect on zeolite 5A is weaker than zeolite 13X. In other words, FAU 13X has a stronger roll-up effect than LTA 5A with the same water vapor content.

It has shown that the adsorption capacity and the affinity of SO₂ depend mainly on exchanged cations of zeolite (Sakizci et al. 2011). At the same time, adsorbate molecule will contact with strong cation center on the zeolite surface first during the adsorption process (Deng et al. 2012). To characterize whether cations and zeolite structure had same impact on roll-up effect, FAU 13X was used for its obvious roll-up effect. According to the different ability to remove cation, hydrochloric and hydrofluoric were used to modify the zeolite at leaching temperature of 30 °C, modification time of 4 h and stirring speed of 100 rpm. The modified zeolite was activated at 300 °C for 2 h. The adsorption characteristics of SO₂ were studied under the conditions: adsorbent 1 g, flow rate 1 L/min, SO₂ 500 ppm, adsorption temperature 30 °C, water vapor 0.9% for HCl-modified zeolite and water vapor 1% for HF-modified zeolite and at 1 atm. The experimental results are shown in Fig. 13. The breakthrough time of modified zeolite decreases with the increase of acid concentration, indicating negative effect of increasing acid concentration on the breakthrough time.

In order to explain this phenomenon, the 13X zeolite was analyzed by XRD. The results shown in Fig. 14 show that acids cause the destruction of crystal structure and the decrease of crystal order. The addition of acid destroyed zeolite structure, which leads to the decrease of the breakthrough time.

However, Fig. 13 shows that hydrochloric and hydrofluoric acid has a different impact on roll-up effect. With increasing acid concentration from 0 to 1 mol/L, the roll-up ratio decreases from 1.74 to 1.07 for HCl-modified zeolite and declines from 2.45 to 1.87 for HF-modified zeolite.

In order to explain the reason of this difference, the 13X zeolite was analyzed by XRF and the results are shown in Fig. 15. It shows the correlation between η and A/S ratio and CaO and Na₂O contents of modified zeolite. The variation of η shows an evident changing trend. When the HCl concentration increases, the S/A increases from 1.77 to 1.88. Conversely, the value of η decreases from 1.73 to 1.07 and the content of CaO decreases from 0.94 to 0.88 wt% and Na₂O decreases from 13.40 to 4.37 wt%, respectively. When the HF concentration

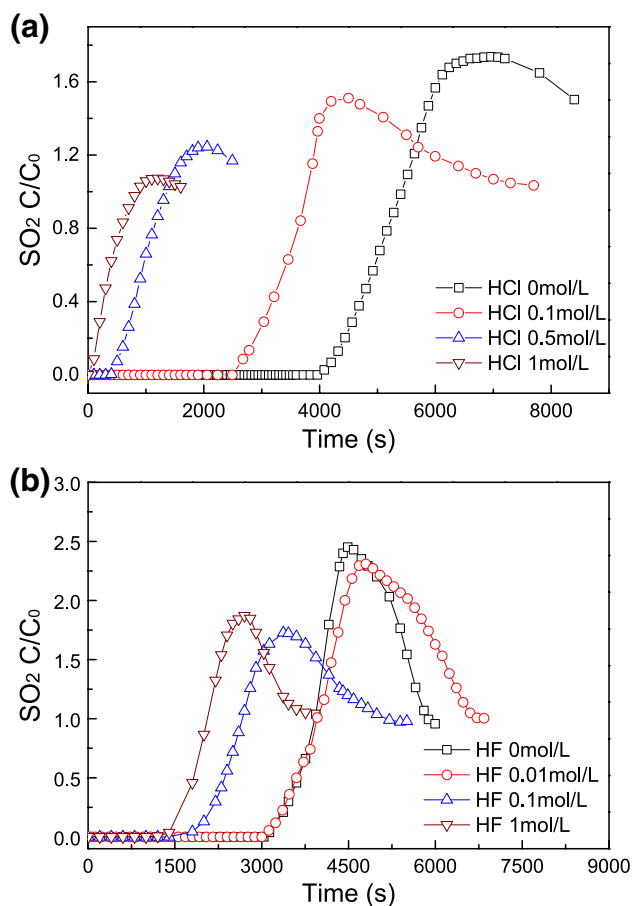


Fig. 13 Effect of acid-treated of zeolites on SO₂ breakthrough curves. **a** Modified 13X by HCl; **b** Modified 13X by HF

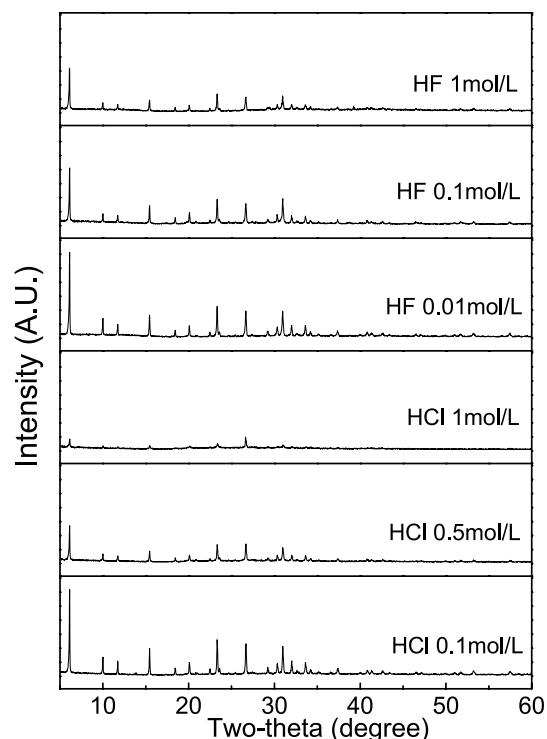


Fig. 14 XRD patterns of zeolite 13X treated by different acid liquor

increases, the S/A decreases from 1.77 to 1.61 and the η decreases from 2.45 to 1.87. Also, the content of CaO increases from 0.94 to 1.01 wt% and that of Na₂O increases from 13.40 to 13.45 wt%. The results show a positive correlation between η and contents of Ca²⁺ or Na⁺. Hence, the cations of zeolite also play an important role in the roll-up effect.

4 Conclusions

FAU 13X and LTA 5A have similar S/A and specific surface areas. Experimental results showed that the roll-up effect is caused by the competitive adsorption of SO₂ and H₂O(g), revealed by different breakthrough rates between H₂O(g) and SO₂. FAU 13X presents a stronger roll-up effect than LTA 5A within the water vapor content range from 0.9 to 2.4%. The minimum water vapor content causing roll-up effect is 1% for LTA 5A and 2% for FAU 13X. The η decreases from 1.23 to 1.02 for LTA 5A and decreases from 1.74 to 1.29 for FAU 13X with the adsorption temperature changes from 30 to 100 °C. Besides, the decrease of gas pressure leads to a reduction in roll-up ratio from 1.23 to 1.05 for LTA 5A and from 1.92 to 1.59 for FAU 13X. The presence of oxygen could increase the SO₂ breakthrough time and diminish the roll-up effect.

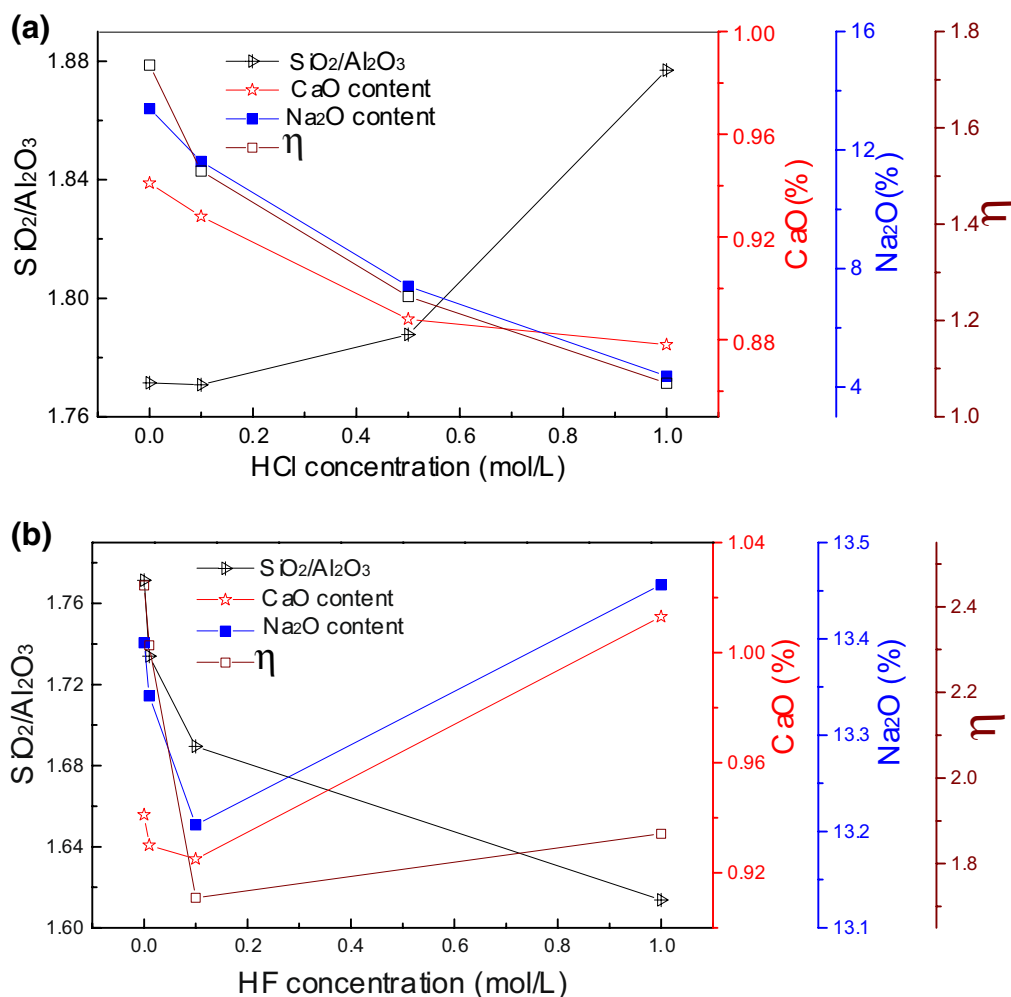


Fig. 15 Influence of acid modification on cation and Roll-up ratio of zeolite. **a** Modified 13X by HCl; **b** Modified 13X by HF

Acid-modified zeolites showed that there is a positive correlation between roll-up effect ratio and content of Ca²⁺ or Na⁺ of zeolites, demonstrating an important role of that cations in the roll-up effect.

Acknowledgements The authors wish to express their thanks to the National Natural Science Foundation of China (Nos. 51234008 and 51174230) for financial support. This work was also financially supported by the Co-Innovation Center for Clean and Efficient Utilization of Strategic Metal Mineral Resources.

References

Al-Harashseh, M., Shawabkeh, R., Batiha, M., Al-Harashseh, A., Al-Zboon, K.: Sulfur dioxide removal using natural zeolitic tuff. *Fuel Process Technol.* **126**, 249–258 (2014)
 Anan, K., Pan, X.C.: Exposure-response functions for health effects of ambient air pollution applicable for China a meta-analysis. *Sci. Total Environ.* **329**, 3–16 (2004)

Barros, M., Zola, A.S., Arroyo, P.A., Tavares, C.R.G., Sousa-Aguilar, E.F.: Chromium uptake from tricomponent solution in zeolite fixed bed. *Adsorption* **12**, 239–248 (2006)
 Bruce, K.R., Gullett, B.K., Beach, L.O.: Comparative SO₂ reactivity of CaO derived from CaCO₃ and Ca(OH)₂. *AIChE J.* **35**, 37–41 (1989)
 Chang, G., Song, C., Wang, L.: A modeling and experimental study of flue gas desulfurization in a dense phase tower. *J. Hazard. Mater.* **189**, 134–140 (2011)
 Deng, H., Yi, H., Tang, X., Yu, Q., Ning, P., Yang, L.: Adsorption equilibrium for sulfur dioxide, nitric oxide, carbon dioxide, nitrogen on 13X and 5A zeolites. *Chem. Eng. J.* **188**, 77–85 (2012)
 Doğu, G., Pekediz, A., Doğu, T.: Dynamic analysis of viscous flow and diffusion in porous solids. *AIChE J.* **35**, 1370–1375 (1989).
 Dunn, J.P., Cai, Y., Liebmann, L.S., Stenger, H.G. Jr, Simpson, D.R.: A test and demonstration unit for concentrating sulfur dioxide from flue gas. *Ind. Eng. Chem. Res.* **35**, 1409–1416 (1996)
 Gupta, A., Gaur, V., Verma, N.: Breakthrough analysis for adsorption of sulfur-dioxide over zeolites. *Chem. Eng. Process* **43**, 9–22 (2004)
 Ishizuka, T., Yamamoto, T., Murayama, T., Tanaka, T., Hattori, H.: Effect of calcium sulfate addition on the activity of the absorbent for dry flue gas desulfurization. *Energy Fuel* **15**, 438–443 (2001)

- Izumi, J., Suzuki, M.: Oxygen selectivity on partially K exchanged Na-A type zeolite at low temperature. *Adsorption* **7**, 27–39 (2001).
- Li, G., Liu, C., Rao, M., Fan, Z., You, Z., Zhang, Y., Jiang, T.: Behavior of SO₂ in the process of flue gas circulation sintering (FGCS) for iron ores. *ISIJ Int.* **54**, 37–42 (2014).
- Marcu, I.C., Sandulescu, I.: Study of sulfur dioxide adsorption on Y zeolite. *J. Serb. Chem. Soc.* **69**, 563–570 (2004)
- Mello, M., Eić, M.: Adsorption of sulfur dioxide from pseudo binary mixtures on hydrophobic zeolites: modeling of the breakthrough curves. *Adsorption* **8**, 279–289 (2002).
- Mofarahi, M., Gholipour, F.: Gas adsorption separation of CO₂/CH₄ system using zeolite 5A. *Microporous Mesoporous Mater.* **200**, 1–10 (2014).
- National Bureau of Statistics of China: China statistical yearbook–2016. China Statistics Press, Beijing (2016)
- Rouf, S.A., Eić, M.: Adsorption of SO₂ from wet mixtures on hydrophobic zeolites. *Adsorption* **4**, 25–33 (1998).
- Sakizci, M., Erdoğan Alver, B., Yörükoğullari, E.: Influence of the exchangeable cations on SO₂ adsorption capacities of clinoptilolite-rich natural zeolite. *Adsorption* **17**, 739–745 (2011).
- Sing, K.S.W.: Reporting physisorption data for gas/solid systems with special reference to the determination of surface area and porosity. *Pure Appl. Chem.* **57**, 603–619 (1985)
- Sotelo, J.L., Uguina, M.A., Águeda, V.I.: Fixed bed adsorption of benzothiophene over zeolites with faujasite structure. *Adsorption* **13**, 331–339 (2007).
- Stenger, H.G. Jr, Hu, K., Simpson, D.R.: Competitive adsorption of NO, SO₂ and H₂O onto mordenite synthesized from perlite. *Gas Sep. Purif.* **7**, 19–25 (1993a).
- Stenger, H.G. Jr, Hu, K., Simpson, D.R.: Chromatographic separation and concentration of sulfur dioxide in flue gases. *Ind. Eng. Chem. Res.* **32**, 2736–2739 (1993b)
- Tantet, J., Eić, M., Desai, R.: Breakthrough study of the adsorption and separation of sulfur dioxide from wet gas using hydrophobic zeolites. *Gas Sep. Purif.* **9**, 213–220 (1995)
- Xiong, Y., Niu, Y., Tan, H., Liu, Y., Wang, X.: Experimental study of a zero water consumption wet FGD system. *Appl. Therm. Eng.* **63**, 272–277 (2014)
- Yang, R.T.: Gas separation by adsorption processes. Butterworth-Heinemann, Oxford (2013)
- Yi, H., Deng, H., Tang, X., Yu, Q., Zhou, X., Liu, H.: Adsorption equilibrium and kinetics for SO₂, NO, CO₂ on zeolites FAU and LTA. *J. Hazard. Mater.* **203–204**, 111–117 (2012)
- Zhang, H., Rao, M., Fan, Z., Zhang, Y., Li, G., Jiang, T.: Effects of circulated flue gas components on iron ore sintering. *ISIJ Int.* **52**, 2139–2144 (2012).
- Zhou, X., Yi, H., Tang, X., Deng, H., Liu, H.: Thermodynamics for the adsorption of SO₂, NO and CO₂ from flue gas on activated carbon fiber. *Chem. Eng. J.* **200–202**, 399–404 (2012)